Electronic Supplementary Material (ESI) for Integrative Biology

Supporting information

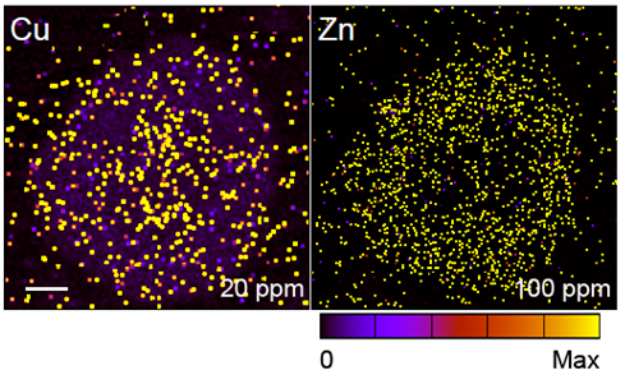

Figure S1. Elemental distributions within DLD-1 spheroid sections obtained using PIXE mapping. PIXE elemental maps (P, S, Cl, K, and Fe) obtained from a cryo-section of a DLD-1 cell spheroid. The maximum element concentration is given at the bottom right corner of each map. Scale bar: 100 µm.

Band Position (cm^{-1})	Assignment	Molecule	Figure 2
2958	$\nu_{as}(CH_3)$ (1)	Proteins, lipids and phospholipids	**E**
1743	ν(C=O) (2,3)	Lipids and phospholipids	**G**
1659	Amide 1 (triple helix)(4)	Collagen	**M**
1656	amide 1 (α-helix) (5)	Peptides and proteins	**C**
1633	amide 1 (β-sheet) (5)	Peptides and proteins	**D**
1621	ν(C=O) (6,7)	Nucleic acid (necrosis marker I)	**L** & O
1467	$\delta(CH_2)$ (2,3)	Lipids and phospholipids	**F**
1234	$\nu_{as}(PO_2^-)$ (8,9)	Phospholipids, nucleic acids	**J**
1128	ν(C-O) (10)	Lactate	**H**
1082	$\nu_s(PO_2^-)$ (8)	Phospholipids, nucleic acids	**I**
1069	ν(C-O-H) (7)	Deoxyribose nucleic acid (necrosis marker II)	**K** & **N**
995	ν(P-O-C) (8,9)	Phospholipids, nucleic acids	Not shown

Table S1. Band assignments for functional group images generated from FT-IR second-derivative spectra. ν – stretching, as – anti-symmetric, s – symmetric, δ - deformation

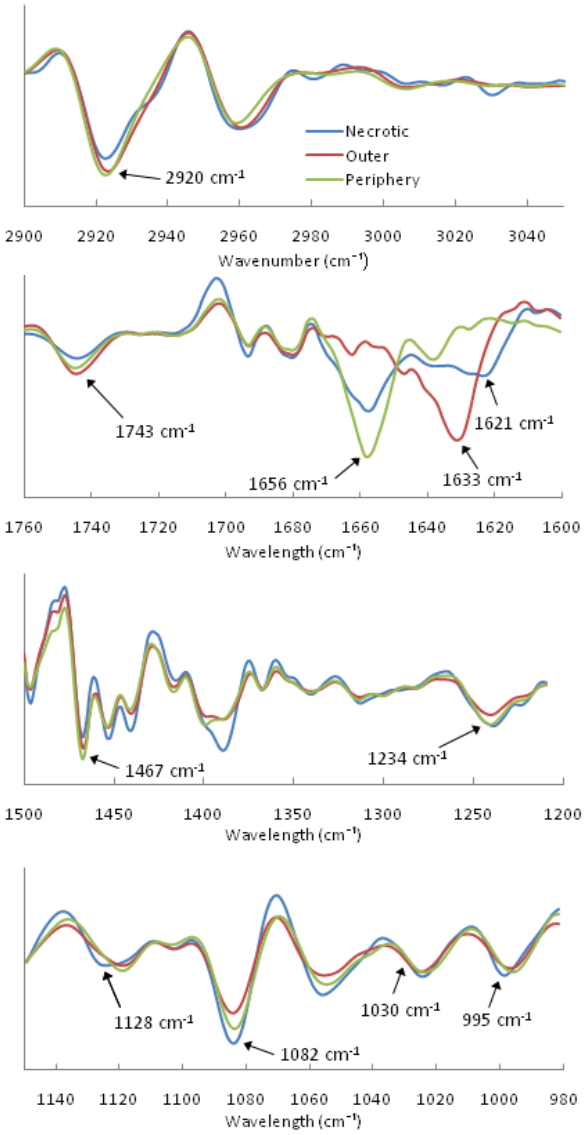

Figure S2. Representative second-derivative FT-IR spectra collected from the necrotic, outer and peripheral regions of DLD-1 cell spheroids.

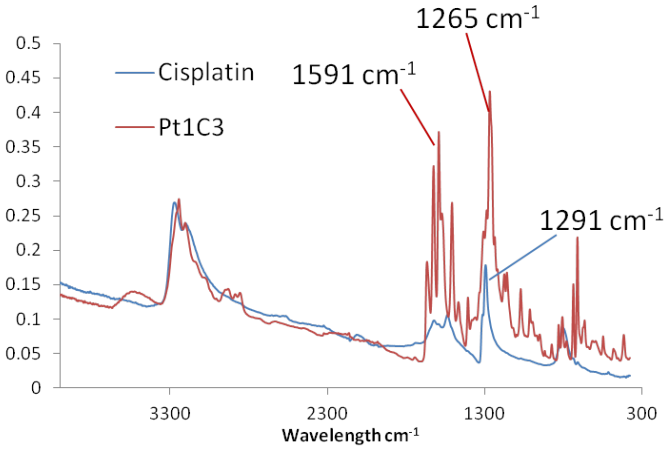

Figure S3. FT-IR spectra of cisplatin and Pt1C3 solids.

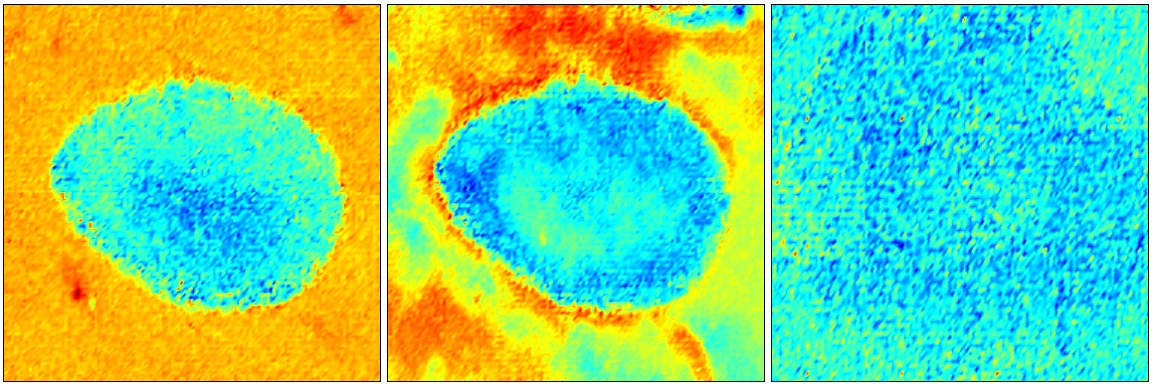

Figure S4. FT-IR maps of treated DLD-1 spheroids: Pt1C3 (10 µM, 24 h) – A: 1591 cm^{-1} and B: 1265 cm^{-1}; cisplatin (30 µM, 24 h) – C: 1291 cm^{-1}. False colour images of a representative DLD-1 cell spheroid cryo-section were constructed by measuring the bands of interest in the second-derivative FT-IR spectra

Supporting References

1. Petibois, C. and G. Deleris. 2006. Chemical mapping of tumor progression by FT-IR imaging: towards molecular histopathology. Trends in Biotechnology 24:455-462.

2. Movasaghi, Z., S. Rehman, and I. Rehman. 2008. Fourier transform infrared spectroscopy of biological tissues. Appl. Spectrosc. Rev. 43:134-179.

3. Wong, P. T. T. and H. H. Mantsch. 1988. High-pressure infrared spectroscopic evidence of water binding sites in 1,2-diacyl phospholipids. Chem. Phys. Lipids 46:213-224.

4. Belbachir, K., R. Noreen, G. Gouspillou, and C. Petibois. 2009. Collagen types analysis and differentiation by FTIR spectroscopy. Analytical and Bioanalytical Chemistry 395:829-837.

5. Pelton, J. T. and L. R. McLean. 2000. Spectroscopic methods for analysis of protein secondary structure. Anal. Biochem. 277:167-176.

6. Gasparri, F. and M. Muzio. 2003. Monitoring of apoptosis of HL60 cells by Fourier-transform infrared spectroscopy. Biochem. J. 369:239-248.

7. Di Giambattista, L., D. Pozzi, P. Grimaldi, S. Gaudenzi, S. Morrone, and A. C. Castellano. 2011. New marker of tumor cell death revealed by ATR-FTIR spectroscopy. Analytical and Bioanalytical Chemistry 399:2771-2778.

8. Wood, B. R., B. Tait, and D. McNaughton. 2000. Fourier transform infrared spectroscopy as a method for monitoring the molecular dynamics of lymphocyte activation. Appl. Spectrosc. 54:353-359.

9. Jamin, N., L. Miller, J. Moncuit, W. Fridman, P. Dumas, and J. Teillaud. 2003. Chemical heterogeneity in cell death: Combined synchrotron IR and fluorescence

microscopy studies of single apoptotic and necrotic cells. Biopolymers 72:366-373.

10. Petibois, C., B. Drogat, A. Bikfalvi, G. Deleris, and M. Moenner. 2007. Histological mapping of biochemical changes in solid tumors by FT-IR spectral imaging. FEBS Lett. 581:5469-5474.